



HAL
open science

Ring shells obtained from pure water drops evaporating on a soluble substrate

Alexandra Mailleur, Christophe Pirat, Gilles Simon, Rémy Fulcrand, Jean
Colombani

► **To cite this version:**

Alexandra Mailleur, Christophe Pirat, Gilles Simon, Rémy Fulcrand, Jean Colombani. Ring shells obtained from pure water drops evaporating on a soluble substrate. *Colloids and Surfaces A: Physicochemical and Engineering Aspects*, 2022, 651, pp.129724. 10.1016/j.colsurfa.2022.129724 . hal-03789726

HAL Id: hal-03789726

<https://hal.science/hal-03789726>

Submitted on 27 Sep 2022

HAL is a multi-disciplinary open access archive for the deposit and dissemination of scientific research documents, whether they are published or not. The documents may come from teaching and research institutions in France or abroad, or from public or private research centers.

L'archive ouverte pluridisciplinaire **HAL**, est destinée au dépôt et à la diffusion de documents scientifiques de niveau recherche, publiés ou non, émanant des établissements d'enseignement et de recherche français ou étrangers, des laboratoires publics ou privés.

Ring shells obtained from pure water drops evaporating on a soluble substrate

Alexandra Mailleur, Christophe Pirat, Gilles Simon, Rémy Fulcrand, Jean Colombani*

Institut Lumière Matière; Université de Lyon; Université Claude Bernard Lyon 1; CNRS UMR 5306; Domaine scientifique de la Doua, F-69622 Villeurbanne, France

Abstract

When a pure water drop evaporates on a soluble substrate, the final ring deposit takes the form of an inclined wall for small and flat drops and of a hollow rim for other geometries. We report here on experiments of evaporation of pure water and salty water drops on salt single crystals and inert substrates, which permit to define precisely the experimental conditions necessary to obtain such structured deposits. Their growth is not a consequence of particular thermal or chemical conditions but of the peculiar geometry of the experiments. Beside the advection of the solute toward the edge by the coffee-stain effect induced by the pinning of the drop, the role of nucleation site played by the salt substrate is a necessary condition for the hollow or inclined rim to appear. These experiments have also shown to which extent the final dryout microstructure is reminiscent of the salt crystallography. Finally, these experiments demonstrate the potentiality of the phenomenon for surface-patterning.

HIGHLIGHTS:

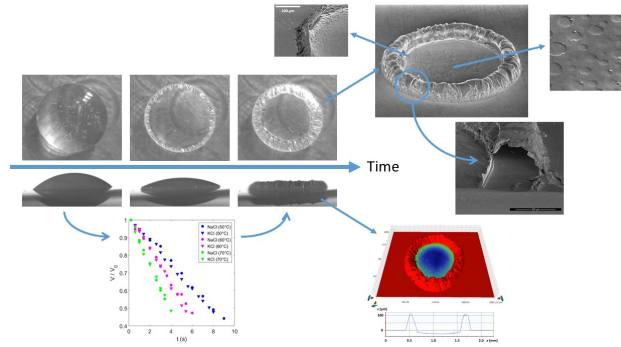
- the evaporation of a pure water drop on a salt substrate leads to a ring deposit
- depending on the drop contact angle the deposit is a hollow rim or an inclined wall
- the evaporation kinetics has no influence on the deposit shape
- the deposit morphology is a consequence of a wetting, evaporation, dissolution, nucleation and growth interaction
- in this configuration new surface patterns may be obtained

*Corresponding author

Email address: `jean.colombani@univ-lyon1.fr` (Jean Colombani)

Keywords: evaporation, pattern formation, salt, coffee stain effect, dissolution, crystal growth.

GRAPHICAL ABSTRACT



1. Introduction

The modeling of matter, through the shaping of volumes or patterning of surfaces, is an ubiquitous feature in geology (stylolites) and biology (biomineralization in shells). Besides, it is also one of the major goals of the material industry, where technical specifications impose given shapes or surface texture to the manufactured products, driven by their function. Field assisted sintering technology (FAST) or large-scale 3D printing are examples of fast evolving shaping techniques; lithography and vapor deposition are constantly improving surface patterning methods.

Among the mechanisms driving surface patterning, the coupling between wetting and growth has aroused a considerable interest lately. In a typical configuration, the fact that the material solidifies or precipitates in a volume constrained by a triple line induces specific, reproducible and possibly complex surface patterns [1]. A particular implementation of this wetting-growth interplay is the formation of a structured stain left by the desiccation of a non-pure liquid drop. Whether the solvent is mixed with a molecular solute or with particles, or with both, its evaporation ends up with the formation of a final deposit [2]. The shape of this deposit derives from the component nature, drop wetting and evaporation kinetics, and ranges from rings [3] to eyes [4], mountains or volcanoes [5], igloos [6], spirals [7], dendrites [8], pillars [9], sombreros [10] or lifted crystals [11].

In the case of a non-heated substrate with pinned triple line and low contact angle, whatever the liquid (colloidal suspension, biological fluid, aqueous electrolyte), the deposit geometry is ring-shaped, the advection of the nonvolatile

component to the drop periphery being driven by a higher evaporation rate close to the triple line [3, 8, 12, 13, 14, 15]. This fundamental feature, often called the coffee stain effect, has been seen to be also valid in the case of non-circular contact lines [16].

While it had been investigated once numerically in the case of microdroplets [17], evaporation on a dissolving substrate had not received any experimental attention until now. We have shown recently that complex and tunable structures may be obtained from the evaporation of a pure water drop, provided that it evaporates on a very soluble substrate, making of this configuration a promising surface-patterning technique [18]. Indeed the coffee stain effect induces here a migration of the components dissolved from the substrate toward the edge of the drop and the eventual growth of an unexpected hollow rim or inclined circular wall.

Whereas these preliminary experiments have shown the potentiality of the technique, the question of the precise experimental conditions leading to these peculiar dried patterns remains open. Therefore, in order to better define the context of appearance of these crystalline rims, but also to better know their crystalline microstructure and their geometric variability, we have carried out new experiments in various conditions, which have brought the following new insights into the phenomenon.

First we show the absence of influence of the evaporation kinetics and evaporation regime on the deposit morphology. Second we define the way the crystalline nature of the grown solid shapes the ring deposit through the central basin texture, the existence of streaks at the rim surface and the presence of step trains at the inner deposit. Third we demonstrate that the presence of dissolved salt in the evaporating solution is a necessary but not sufficient condition for the hollow or inclined rim to grow. Indeed the salt substrate plays the role of a nucleation site, indispensable for obtaining a peripheral deposit. Fourth a comparison between two different chloride salts shows that the salt nature has a negligible influence on the deposit morphology. Finally we introduce the large potentiality of this method of surface-patterning, presenting some original obtainable deposit shapes.

2. Material and methods

The salt substrates are NaCl or KCl single crystals, polished with grit size down to 1 μm , in order to provide a reproducible and controlled surface texture. Their dimensions are $10 \times 10 \times 1 \text{ mm}^3$. The substrates are placed in notches etched in a copper plate, heated with thermal resistances. The temperature of this metallic base is regulated via platinum probes and fixed between 20 and 80°C.

Ultra pure water drops of volume ranging from 0.05 to 3.5 μL are deposited with a syringe driver and observed from the top and the side by cameras. The volume of the drop is computed with an image processing software in two ways: from the hanging droplet before deposition, and from the initial spherical cap shape of the sessile drop, to check the measurement consistency.

The whole setup is located inside a closed box where the hydrometry is controlled thanks to a saturated salt solution poured a wide beaker. With this system, we obtain a relative humidity between 18 and 45%.

The variability of the deposit morphology has been tested in modifying the temperature, relative humidity, drop initial volume and initial contact angle. The deposits after complete drying have been observed by scanning electron microscopy (SEM) in vacuum, to get three-dimensional views of their geometry. Quantitative measurements have been obtained in carrying out systematically vertical scanning interferometry (VSI) measurements in air regarding the rim height, drop sessile diameter and digging depth.

3. Results and discussion

3.1. Evaporation kinetics

Before investigating the ring-like dryout, we first characterize the kinetics of evaporation, in order to situate our study among the numerous studies of drop evaporation [19]. Fig. 1 displays the evolution with time t of the volume V of droplets, normalized by their initial volume V_0 , for various temperatures, before the triple line recedes (see section 3.2). The initial volumes are of the order of half a μl . All curves show a linear behavior, whatever the temperature, corresponding to a constant evaporation rate dV/dt in the first stage of evaporation. This is a characteristic feature of the pinned regime for contact angles less than 40° [20].

As expected, the slope of the straight lines, so the evaporation rate, increases with temperature (Fig. 1). For negligible temperature gradients between the liquid and the surrounding atmosphere, a pure diffusive transport of the water vapor from the drop free surface is expected. In this case, when the substrate is not heated, an analytic model of the drop volume V evolution has been proposed by Hu & Larson [20]:

$$V/V_0 = 1 - (RD_v(1 - H)c_v/\rho)t \quad (1)$$

where D_v is the diffusion coefficient of the vapor in air, R the drop base radius, H the relative humidity, c_v the saturated water vapor concentration and ρ the water density. As shown in Fig. 2, the experimental normalized volume evolution (symbols) of two drops with different radii show an excellent agreement with the prediction (dashed lines) without any fitting parameters. This proves that the non-heated pinned drops evaporate in a purely diffusive regime.

We would like to stress on the fact that the c_v and ρ used correspond to the values of saturated salt water, not pure water, and that D_v is dependent on the temperature (see values in the caption of Fig. 2).

When the underlying substrate is heated, a destabilizing temperature gradient between the drop and the environment builds in. In this condition, a convection loop is liable to appear above the drop, and the evaporation is likely to proceed in a non-diffusive regime. To check this assumption, Fig. 3 shows

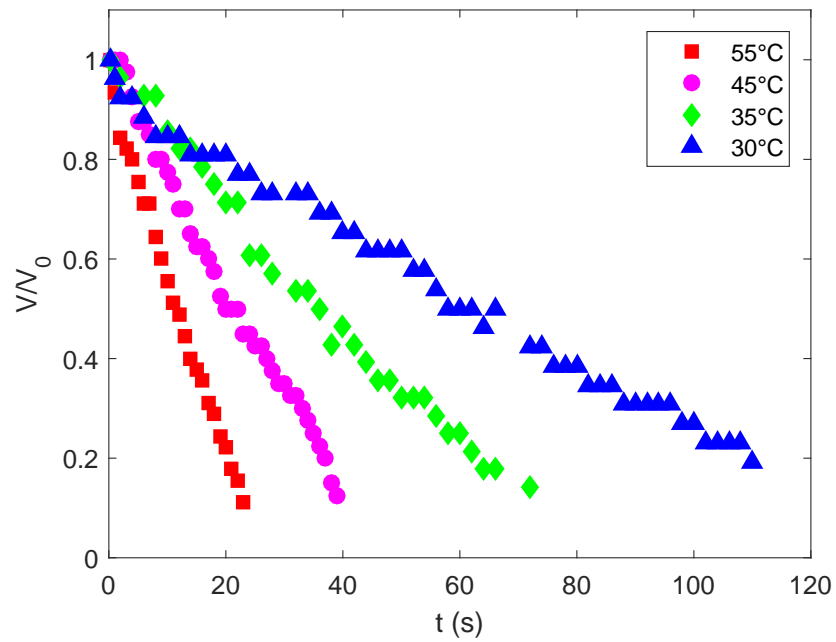


Figure 1: Reduced volume versus time of droplets of pure water evaporating on polished NaCl single crystals, in the pinned triple line regime, for various substrate temperatures.

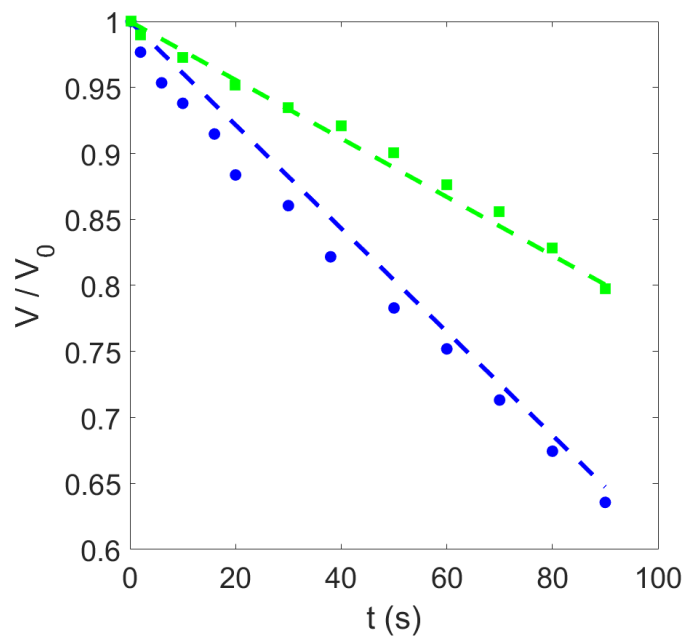


Figure 2: Time evolution of the reduced volume of water drops of sessile radius 0.7 mm (blue circles) and 0.9 mm (green squares) evaporating on a NaCl crystal at 22°C and 45% of relative humidity, and analytic model (dashed line, equation 1) of purely diffusive evaporation of drops of similar radii, with $D_v = 2.43 \times 10^{-5} \text{ m}^2/\text{s}$, $c_v = 1.1 \times 10^{-2} \text{ kg}/\text{m}^3$ and $\rho = 889 \text{ kg}/\text{m}^3$.

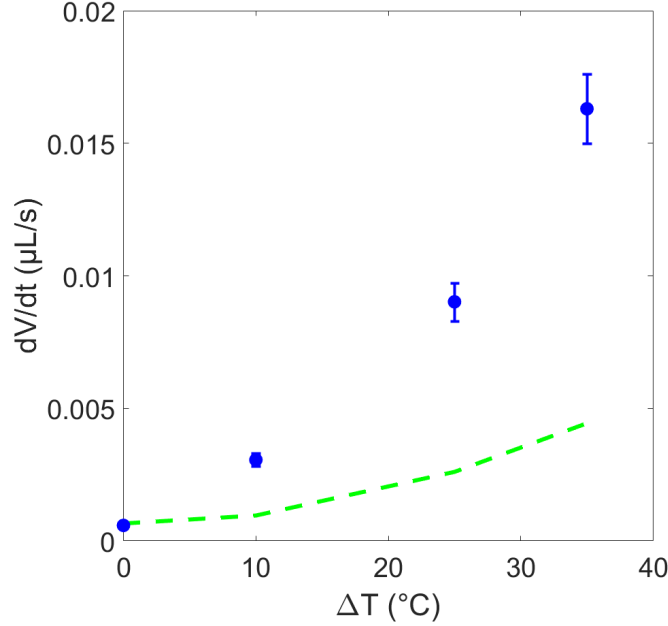


Figure 3: Initial evaporation rate dV/dt of water drops desiccating on a NaCl crystal as a function of the temperature difference between the heated substrate and the surrounding air. The blue dots are experimental data and the green dashed line is the prediction of a purely diffusive model (equation 1). The sessile diameter of the investigated drops is comprised between 1.6 and 1.8 mm.

the initial evaporation rate dV/dt , computed from the initial slope of the volume evolution curve, and its analytic prediction, computed from equation 1, for various substrate-air temperature differences ΔT . In case of homogeneous temperature, the experimental and theoretic values collapse, as in Fig. 2, proof that the evaporation is purely diffusive. But as soon as ΔT departs from zero, the experimental data do not fit anymore to the analytic ones, with a discrepancy growing when the thermal gradient rises. This increasing gap between the experimental rate and the prediction of the diffusive model can be attributed to the rising contribution of convection to the water vapor flow from the drop surface [21].

3.2. Shell formation scenario

As soon as the drop is deposited on the salt substrate, evaporation proceeds through diffusion or diffusion-convection in the surrounding air (see section 3.1) and the stain forms in four steps:

1. The evaporation starts in the pinned contact line regime with a decrease of the contact angle accommodating the water loss. A few seconds after

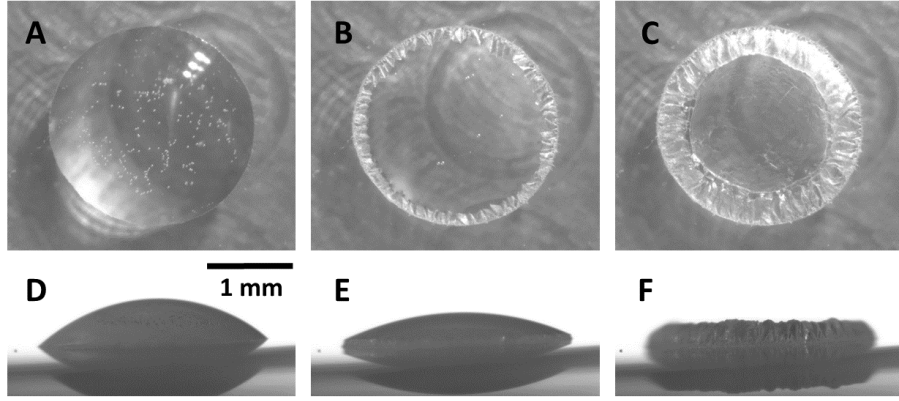


Figure 4: Top (A, B, C) and side (D, E, F) view of the evaporation of a 2.7 mm sessile pure water drop on a NaCl single crystal at 60°C and 30% of relative humidity at elapsed times 2 s (A and D), 45 s (B and E) and 90 s (C and F) s after deposition.

the deposition, a salt solid ring nucleates at the drop contact line and grows continuously, following the drop free surface (Fig. 4 A and D).

2. As soon as the solid grows from the periphery, the contact line leaves the initial drop perimeter and follows the growing shell (Fig. 4 B and E).
3. At the end of the evaporation, the apex of the drop reaches the floor and a new three-phase line is therefore created in the middle of the drop, and recedes outward, until it reaches the inner ring deposit (Fig. 4 C and F).
4. At the very end of the experiment, two types of behavior can be encountered, once all the visible liquid has disappeared: either the shell is open and the experiment stops, or the desiccation continues actually *inside* the closed shell, and an inner triple line recedes slowly until complete evaporation (see Fig. 5).

Therefore two deposit shapes are observed, presented in Fig. 6: either open, when the shell takes the form of walls inclined toward the interior of the drop, or closed, when it resembles a half torus. This latter deposit has the particularity to be hollow. Indeed, a slicing of the deposit reveals that it is a simple closed shell, containing a wide void. The shell is made of a salt wall the thickness of which has been observed to be quite constant for all drop diameter and temperature (see Fig. 7) [18].

We have interpreted the growth of this open or closed rim as the consequence of the following mechanisms [18]. In a few seconds, the dissolution of the substrate below the drop induces a saturation of the water in NaCl (see section 3.3 for details). As the triple line is pinned, an outward capillary flow continuously transfers ions from the center to the edge to compensate the water loss by evaporation [22]. The maximal evaporation at the periphery and the continuous supply of dissolved matter by the advecting flow leads the supersaturation to be the highest at the drop edge, which triggers precipitation at

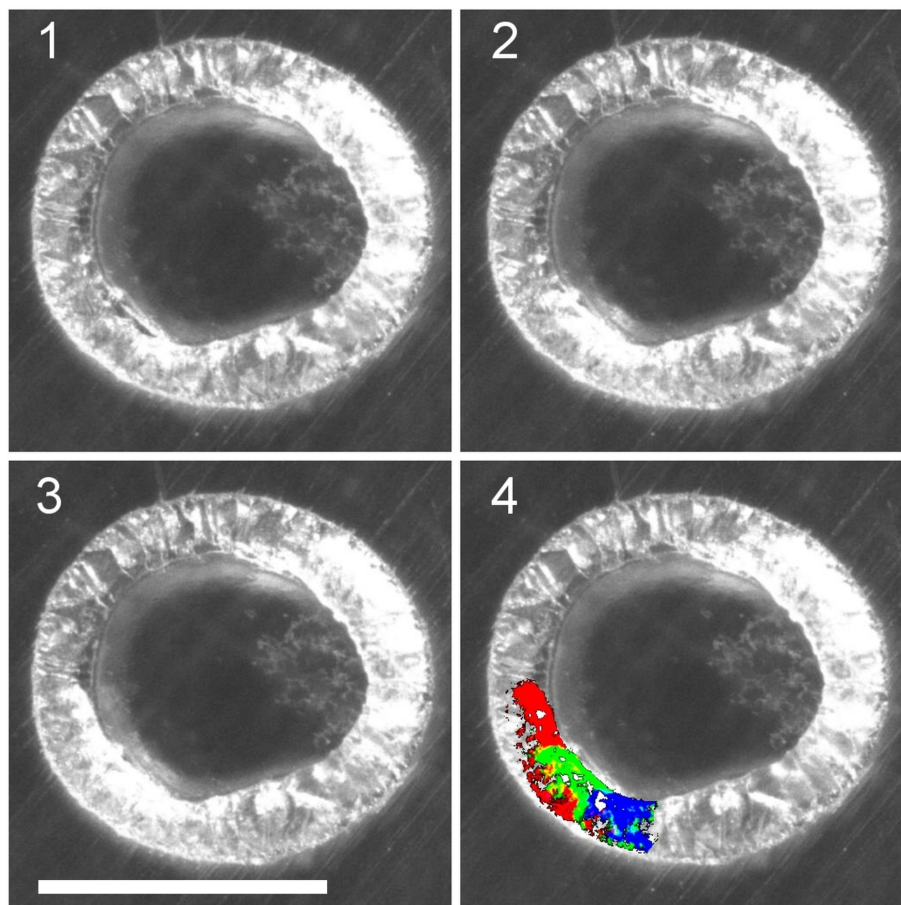


Figure 5: Receding of the triple line inside the deposit at the end of the evaporation of a pure water drop on a KCl single crystal at 71.5°C and 29% of relative humidity. For a better clarity, the last image gathers the successive front advances with different colors, in a blue-green-red sequence. The white scale bar length is 1 mm.

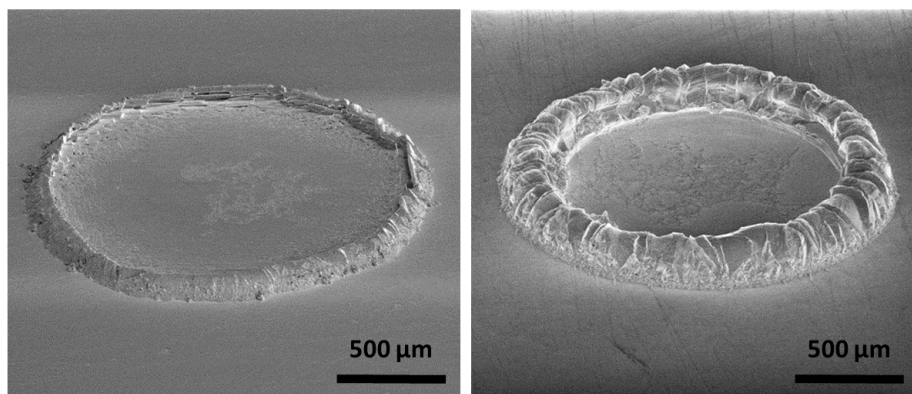


Figure 6: SEM images of the two characteristic morphologies of the final ring deposit of a water drop evaporated on a NaCl single crystal: inclined walls (left) and half-torus (right).

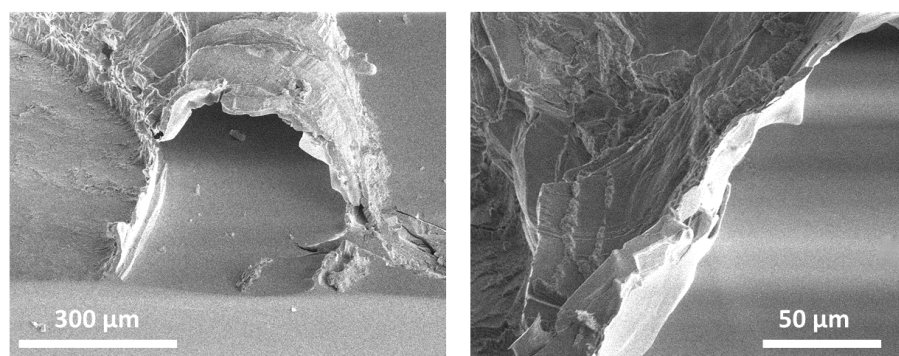


Figure 7: SEM images of the hollow shell from which the half-torus morphology of figure 6 is made (left) and closeup of this shell (right).

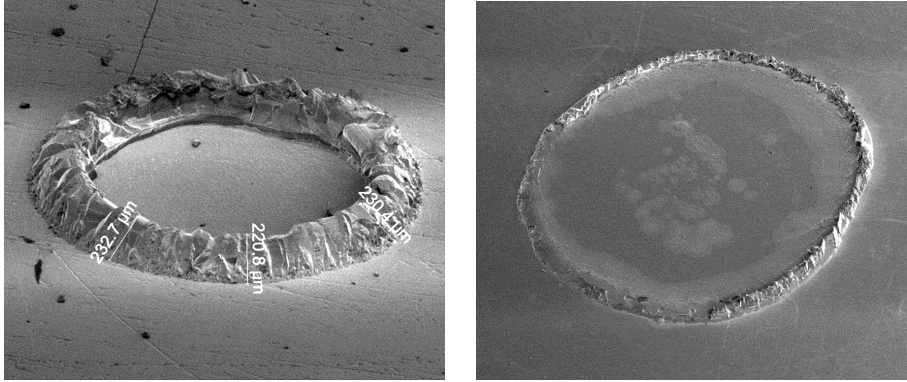


Figure 8: SEM images of the final deposit obtained after evaporation on a salt crystal of two water drops of similar sessile diameter (2.2 mm left and 1.7 mm right), at similar temperature (55°C and 50°C) and similar relative humidity (26% and 24%) but initial contact angle strongly different: 31° for the closed shell in the left image and 11° for the open shell in the right image.

the triple line. More precisely, the initial deposit is probably shaped by the competition between this advective flow and an adverse diffusive flux induced by the resulting peripheral buildup of solute [23].

Subsequently the triple line follows the growing shell. The continuous lowering of the free surface induces a progressive curvature of the shell. In most cases, the shell continues to grow during the receding of the inner triple line, formed when the apex has reached the drop bottom, and closes. When the drop is particularly flat (small contact angle) or small (low sessile diameter), the evaporation duration is too short, the growth stops before the shell closure, and the rim remains open.

In the analytic model developed in reference [18], the temperature, so the evaporation rate, does not influence the deposit morphology and only changes the shell formation kinetics. Fig. 8 displays two deposits of similar diameters, obtained in similar temperature and humidity conditions, but one with a contact angle three times higher than the other. The resulting shell happens to be closed for the most convex drop, whereas it has remained open for the flattest one, showing how the drop geometry is the driving parameter of the morphology selection.

The modification of the evaporation process from diffusive to diffusive-convective, noticed in section 3.1, is therefore viewed to have no influence on the deposit morphology.

3.3. Details of the deposit morphology

The profilometric view of a characteristic deposit is displayed in Fig. 9. The depression in the center of the final stain is seen to exhibit a quasi parabolic shape. To help the interpretation of this geometric feature, we have performed

the following experiment. A water drop is deposited on a salt substrate at ambient temperature, but it is subsequently dried with a wipe 10 s after deposition. It is observed that the central etching already exists after this shortened drying. Although the exact dissolution rate of NaCl is not known, it is accepted that its dissolution is fast enough for being always diffusion-driven, i.e., the mass transport of the released ions in the liquid is so slow compared to the chemical reaction that it controls the whole kinetics [24]. Therefore the characteristic dissolution time is given by the diffusion time of the dissolved salt in the drop $\tau \sim h^2/D$ with h the drop height and D the diffusion coefficient of the salt ions in water. Using $h \sim 100 \mu\text{m}$ and $D \sim 10^{-9} \text{ m}^2/\text{s}$, one can consider thereby that the drop water saturates in $\tau \sim 10 \text{ s}$. Consequently theory and experiment agree on the fact that the central depression forms in the very beginning of the evaporation. The parabolic shape of the substrate can be viewed as the mirror of the drop shape, the larger water height above the solid leads to a higher dissolution before reaching the saturation and therefore a deeper etching.

Beyond the overall parabolic retreat of the surface, the dissolution process at the local scale is heterogeneous. Fig. 10 shows the SEM picture of the dryout center of a pure water drop, where holes are scattered on the surface. Such irregularities are always present, with a variable shape and disposition. Whereas no investigation of the atomic mechanisms of dissolution of sodium chloride crystals in water currently exists, we can propose a probable origin of these holes. Dissolution of minerals proceeds mainly via the migration of atomic steps originating from etch pits, which generally nucleate at crystal defects, mainly vacancies, line dislocations and crystal edges [25]. These steps sweep the reacting surface and disappear by merging with other steps, or by reaching a crystal edge. In fast dissolving minerals, the motion of the steps is too quick, compared to their nucleation rate, for the etch pit to grow deeply [26]. Therefore, encountered etch pits are generally shallow, and are not always reminiscent of the crystalline structure [27, 28]. It is likely that the non-square holes observed in Fig. 10 are such shallow pits. Nevertheless further studies devoted to the atomic mechanism of salt dissolution are necessary to definitely confirm this interpretation.

The general aspect of the deposit is a ring, either open or closed, and the local texture of the grown shell is quite irregular, as can be seen in the closeup of Fig. 7. But the deposit always exhibits a structure at an intermediate scale, with a regular array of streaks etching the shell. These stripes are roughly radial, but a slight anisotropy can be observed, that seems to favor two perpendicular directions, as shown in Fig. 11. Whereas this structure deserves a study in itself, this organization finds its probable source in an adaptation of the growth of the face-centered cubic lattice of NaCl to the constraining circular geometry of the drop.

We have noticed that in some rare cases, crystallites exhibiting a nearly perfect cubic lattice grow at the rim, building hollow cubes among the regular streaks, as displayed in 12.

Beside the parabolic shape of the dryout center, the existence of shallow pits at its surface, and the presence of crystallography-deriving streaks on the

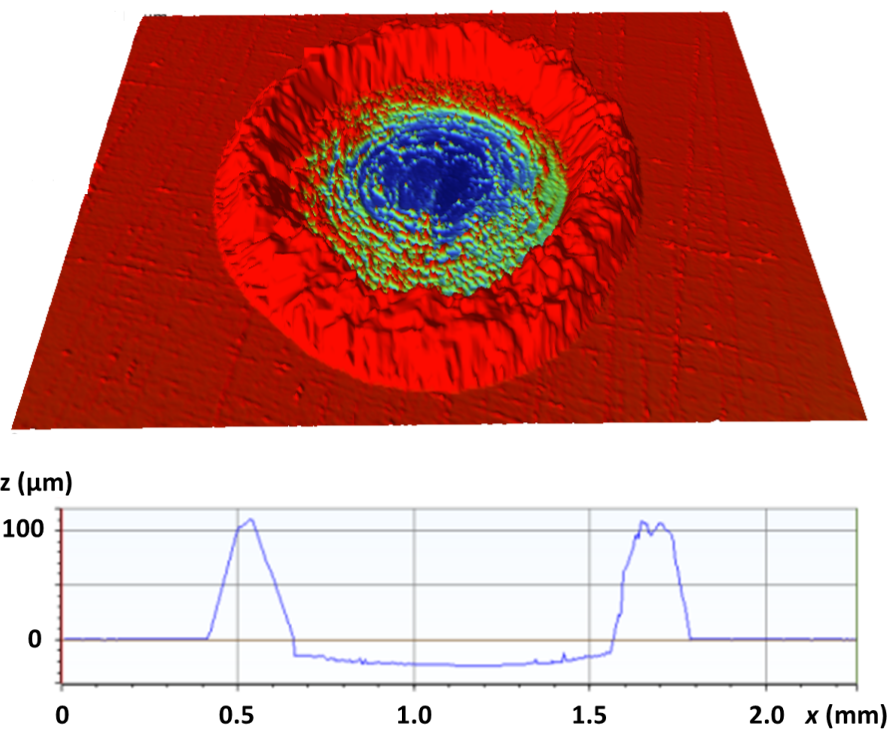


Figure 9: Three-dimensional and two-dimensional profilometric views obtained by VSI of the dryout left by the evaporation of a pure water drop of 1.42 mm sessile diameter at 71°C and 11 % of relative humidity on a NaCl single crystal. This observation emphasizes the regular half-toric shape of the rim, of outcropping height $\sim 120 \mu\text{m}$, and the parabolic etching of the central part, of depth $\sim 10 \mu\text{m}$. The size of the area scanned in the top image is $2.23 \times 1.70 \text{ mm}^2$.

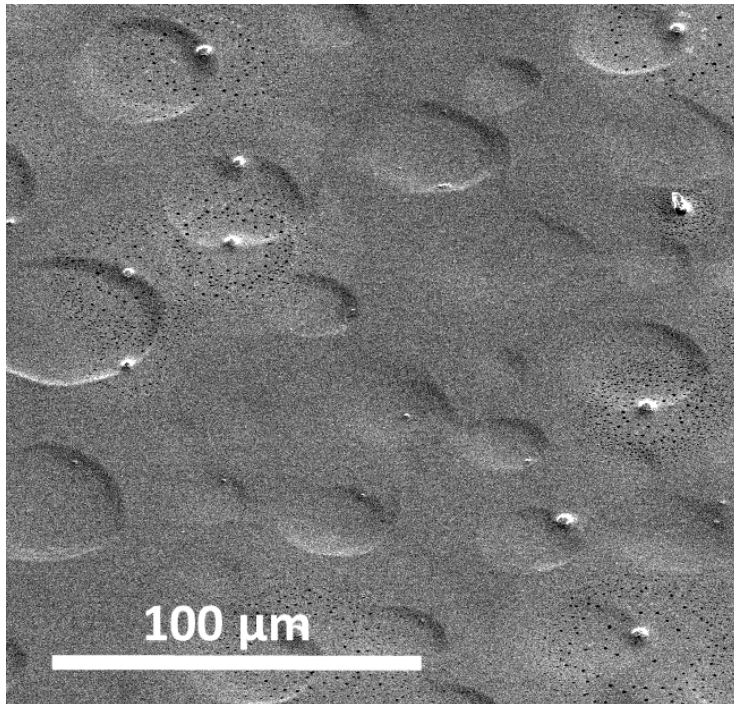


Figure 10: SEM image of the middle of an evaporated water drop on a NaCl crystal. Holes can be seen all across the surface, which are likely to be dissolution etch pits.

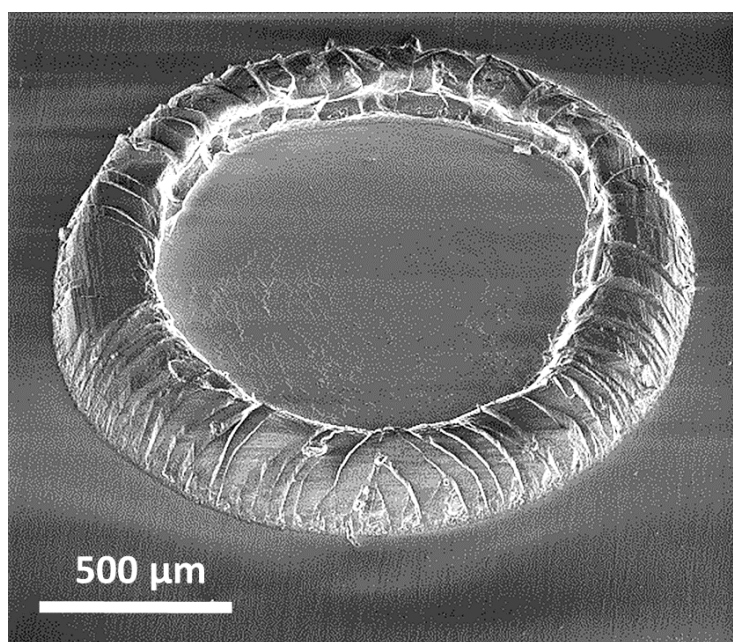


Figure 11: SEM image of the deposit formed by the evaporation of a water drop of sessile diameter 1.8 mm at 61°C and 11% of relative humidity on a NaCl substrate, where the anisotropic network of streaks at the shell surface is clearly visible.

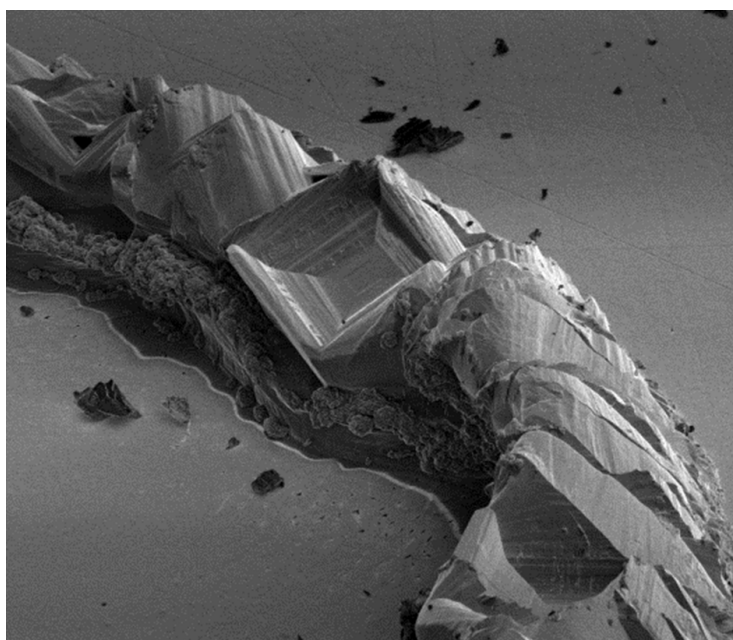


Figure 12: SEM image of the ring deposit of an evaporated water drop of 1.4 mm sessile diameter on a NaCl crystal at 50°C and 26% of relative humidity. The size of the image is $440 \times 390 \mu\text{m}^2$. A cubic crystallite has grown in the middle of the closed rim.

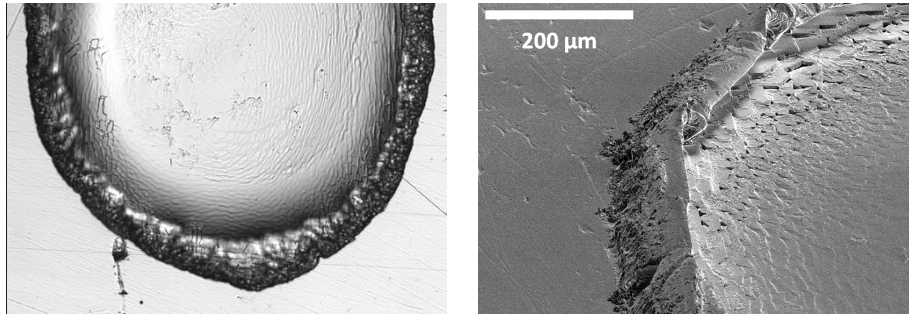


Figure 13: Left: White light observation with a confocal microscope of step bunching (black ripples close to the ring shell) during the evaporation of a water drop of 1.43 mm sessile diameter on a NaCl substrate at 45°C and 40% of relative humidity 39 s after the drop deposition. Right: SEM image of the shell after complete evaporation, with probable remains of a step train at the inner border of the deposit.

shell, a fourth geometric feature has been observed in some experiments. As shown in Fig. 13, macroscopic steps appear at the substrate surface during the evaporation in the vicinity of the growing ring shell. These steps migrate inward at a velocity of the order of $0.1 \mu\text{m/s}$. At the end of desiccation, some irregular steps remain at the shell inner border, whereas all other steps have disappeared. This process is reminiscent of the phenomenon of step bunching observed during crystal growth in a flow along an inclined substrate, where a step train is observed to be created and dragged by a downhill flow, whereas no step exist in an upstream flow [29]. If the origin of the step bunching observed during our experiments is equivalent to the one of this study (crystal growth along a slope in a flow), it informs us that the flow taking place at the solid-liquid interface at the beginning of the evaporation should be inward, outward flow producing no step bunching.

3.4. Variability of the pattern

Our surface patterning experiments are characterized both by the use of an initially pure liquid for the drop and of a dissolving solid for the substrate. In order to check the respective importance of these two features on the final deposit morphology, we have adopted the following design of experiment. Experiments were carried out using the three possible couples: pure liquid/soluble substrate, non-pure liquid/soluble substrate and non-pure liquid/inert substrate, the association pure liquid/inert substrate bringing obviously no deposit:

Pure liquid/soluble substrate : this configuration has been achieved in evaporating drops of pure water on a NaCl substrate, and has been described in detail in section 3.2.

Non-pure liquid/soluble substrate : These conditions have been met in evaporating drops of salty water on a salt substrate, the salt being in

both cases sodium chloride. The concentration of salt in the solution has been chosen quite close to the saturation concentration of NaCl in water, in order to promote the crystal growth. A profilometric observation of a typical dryout is shown in Fig. 14, and SEM images are displayed in Fig. 15. The deposit morphology is seen to be strictly equivalent to the case with pure water, with a hollow ring shell surrounding a central basin. There are two only observable differences. First the surface texture of the grown crystal is very rough, instead of being quite smooth with pure water, making in particular the cavity less regular. Thus the quasi-saturation of the solution seems to promote multiple nucleation sites at the shell surface. Second the central part of the dryout is no more etched in the substrate but is raised above the initial floor level. This shows that the dissolution of the substrate is absent or minimal.

Non-pure liquid/inert surface : The evaporation of saline water on an inert substrate has been realized in desiccating salty water, again with a concentration close to the solubility of NaCl in water, on a silicon wafer. Fig. 16 shows that the final deposit is completely different from the soluble substrate case. As has already been observed [30, 31], there is no coffee-stain here and the dryout is mainly made up of large cubic crystals agglomerated in the center of the stain. During the phenomenon, the nuclei are observed to form in the bulk liquid and are pushed toward the center of the drop during evaporation by the shrinking free surface (see Fig. 17).

We attribute the huge morphology difference between the inert and soluble substrate to the preferential nucleation site of the crystal. In case of dissolution on an inert substrate, it has been argued that sodium chloride precipitates preferentially in contact with a nonpolar medium like air [30]. Thus the nuclei appear at the liquid free surface close to the drop edge, where the supersaturation is maximum. Subsequently, floating in the liquid, they are pushed toward the drop center because of the deformation of the free surface they provoke during its progressive shrinking [31]. If the solvent is more viscous, e.g., a solution of gelatin, the crystallites are seen to stay mainly at the periphery, the viscous forces probably exceeding the capillary forces [32]. For the evaporation on a substrate made of the same ions as the ones present in the solution, either initially (salty solution) or provided by dissolution (pure water), the surface is obviously the most favored site of heterogeneous crystallization. The supersaturation is the highest at the periphery, therefore the nuclei form at the salt surface close to the drop edge, and grow following the three-phase line, building a 'skin' at the free surface, that results in a thin shell, in a process reminiscent to epitaxial growth. Beside wetting and growth, nucleation, precisely the location of nucleation, has therefore a paramount influence on the final pattern.

To get a first idea of the possible influence of the salt nature on the final deposit, experiments have been carried in the same conditions using a NaCl and a KCl substrate. Both salts have a very similar solubility in water (~ 350 g/L)

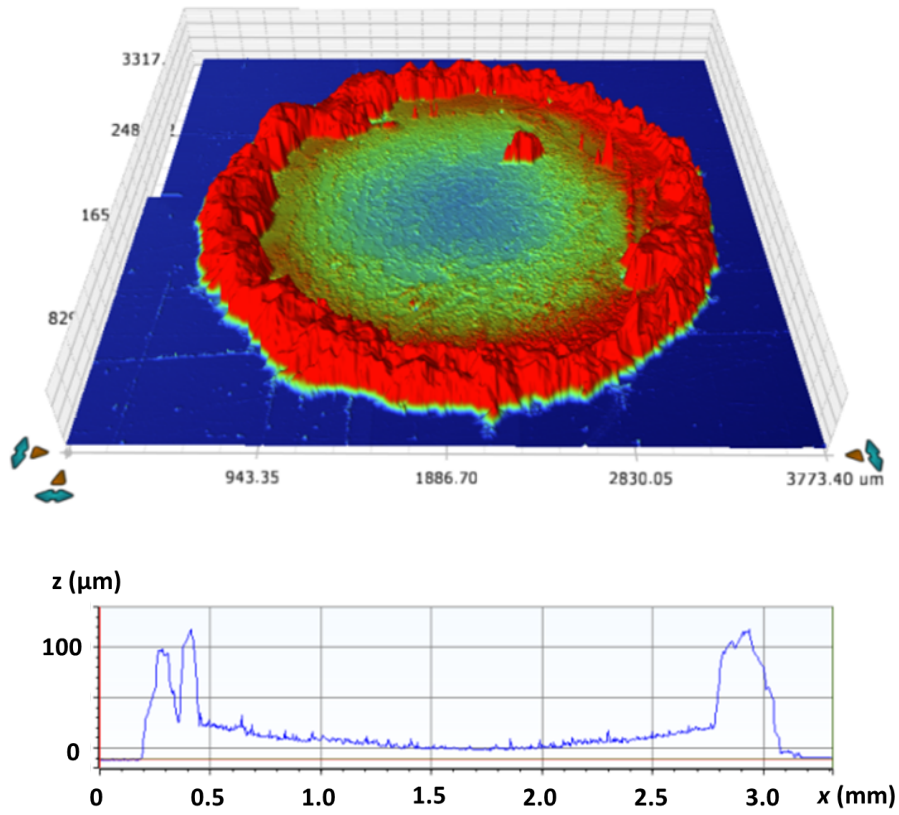


Figure 14: Three-dimensional and two-dimensional profilometric views obtained by VSI of the deposit left by the evaporation of a 2.95 mm sessile diameter drop of saline solution, with a concentration of 90% of the solubility of NaCl in water, on a NaCl single crystal at 25°C. The ring deposit peaks at 240 μm . Contrary to the case of pure water drops (Fig. 9), the substrate inside the drop is not etched, with an altitude higher than the altitude of the substrate outside.

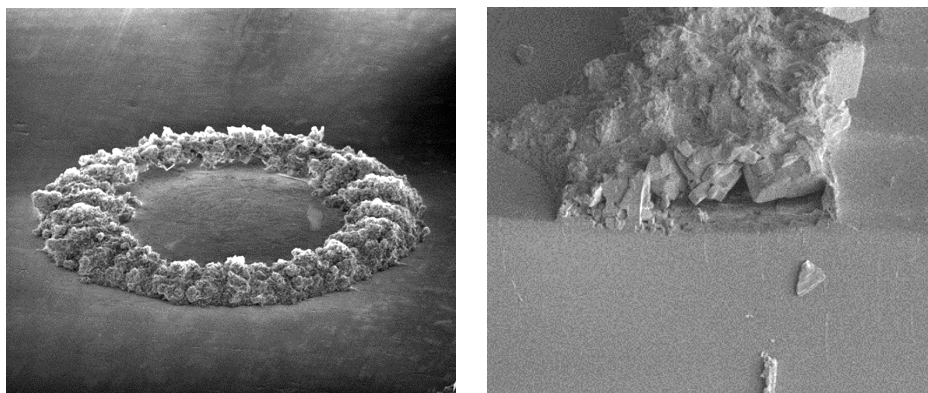


Figure 15: Left: SEM view of the deposit left by the evaporation of a 2.4 mm sessile diameter drop of saline solution, with a concentration of 70% of the solubility of NaCl in water, on a NaCl single crystal at 35°C. Right: cut shell in the same configuration, for a 2.95 mm diameter, a concentration of 90% of the NaCl solubility and a 35°C temperature.

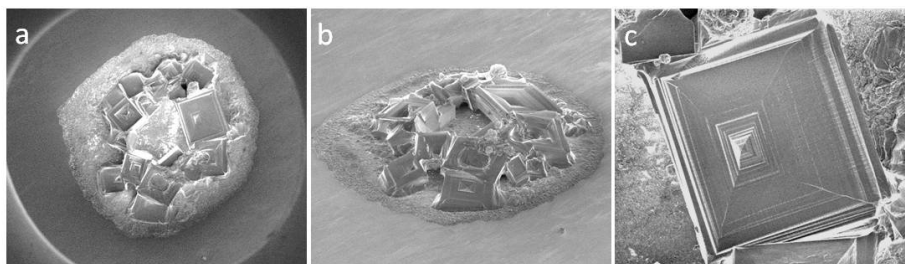


Figure 16: SEM images of the final deposit after evaporation of salty water, with a concentration of 70% of the solubility of NaCl in water, on a silicon wafer at 35 °C and 40% of relative humidity.

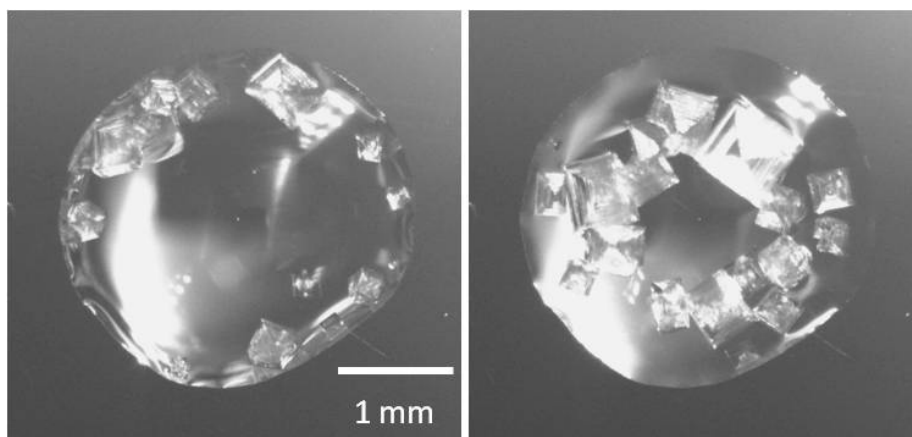


Figure 17: Inward motion of crystallites during the experiment of figure 16.

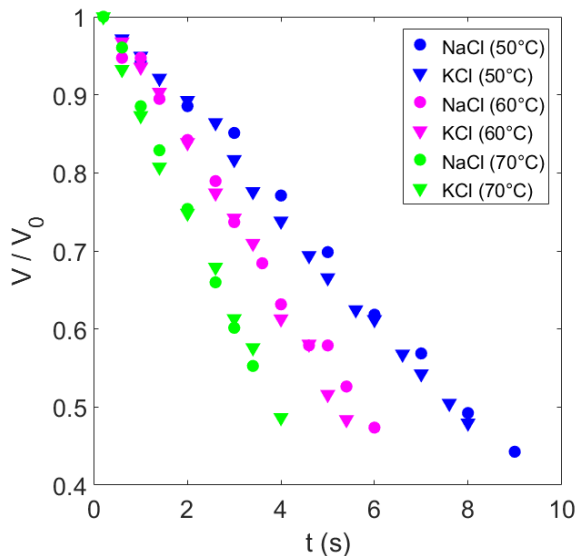


Figure 18: Evolution with time of the reduced volume of drops of sessile diameter 1.2 mm desiccating on NaCl and KCl substrates at 50, 60, and 70°C.

and show a face centered cubic Bravais lattice in the solid state. Therefore no significant effect is expected both on the evaporation kinetics, related to the first phenomenon, and on the deposit morphology, linked to the second characteristics. Fig. 18 confirms that the evaporation rate of a water drop on both a NaCl and a KCl substrate is strictly equivalent for the 3 investigated temperatures, provided that the other parameters are equal. Fig. 19 clearly shows that the stain morphology obtained with these two chloride salts are indistinguishable, both exhibiting the hollow rim shape with regular radial streaks. Therefore we can conclude from this comparison that no forgotten characteristics of the salt influences the deposit shape, which seems to be controlled before all by the wetting, nucleation and growth conditions. Obviously a more comprehensive test of the influence of the nature of the salt, in testing salts other than chloride, is necessary to strengthen this conclusion.

The particular configuration of a pure solvent drop evaporating on a dissolving substrate, compared to the usual configuration of a solvent containing a solute desiccating on an inert substrate, has led to the original shape of a hollow final deposit. Whereas hollow crystals of sodium chloride already exist, with potential pharmaceutical applications [33], no surface pattern with empty cores had been manufactured so far. This kind of geometry may broaden the type of surface pattern achievable industrially. In the particular case of sodium chloride, such hollow structures may be valuable in the food industry, lowering the salt content while maintaining a high salting intensity [34].

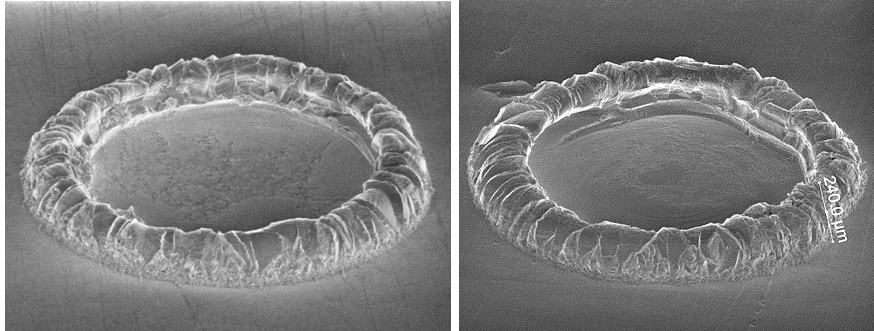


Figure 19: Final ring deposit of water droplets of sessile diameter 1.6 mm evaporating at 56°C on a NaCl (left) and KCl (right) substrate.

To enhance the interest of this novel patterning method, an extension of the variety of obtainable geometry would be beneficial. As a first attempt to widen the applicability of the technique, we review here some original deposit shapes obtained accidentally during our experiments. In Fig. 20a, due to the wetting of the drop along surface scratches, the final deposit exhibits a square shape. In Fig. 20b an inner ring is present inside the main ring. In Fig. 20c, an interlacing network of inner rims is present inside the hollow ring deposit, sharing the central depression in several parts. Finally in Fig. 20d, an external protuberance has grown from the hollow shell, slightly extending the salt crystal outside the ring. All these geometries give a first idea of the diversity of obtainable deposits, that may be extended for example in pre-etching the substrate in order to get a tailored contact line, or in optimizing the parameters in order to obtain a given volume of the hollow core.

4. Conclusion

The evaporation of a drop of pure water on a salt substrate leads to the formation of a ring deposit. Depending on the drop sessile diameter and initial contact angle, this shell takes the form of inclined walls or of a hollow rim. This geometry has been interpreted as the consequence of the deposit growth at the moving triple line, fitting closely the edge of the drop free surface. The smallest and flattest drops exhibit open shells because the desiccation finishes before the shell has had the time to close. We have shown here that both (i) the existence of this shell and (ii) the selection of the open or close morphology, do not depend on the temperature of the substrate (between 20 and 80°C), on the relative humidity (between 18 and 45%), on the evaporation rate (between 6×10^{-4} and 1.6×10^{-2} $\mu\text{L/s}$), on the evaporation regime in the surrounding air (diffusion and/or convection), and on the type of growing chloride salt (NaCl and KCl).

This kind of well-structured deposit is in striking contrast with the close situation of evaporation of saline water on an inert substrate. In this case,

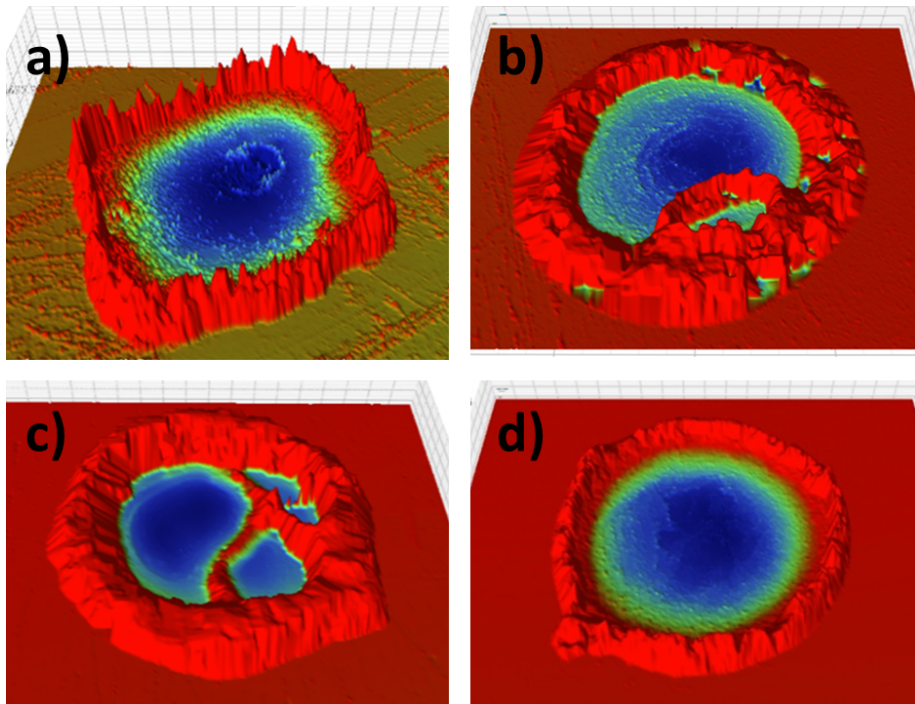


Figure 20: VSI images a) of a square outer rim, b) of an inner rim inside the main rim, c) of an outer rim with inner ramification and d) of an outer rim with protrusion, obtained from the evaporation of a drop of pure water on a salt crystal.

the salt also grows at the drop free surface, but as it does not nucleate at the initial triple line, pinned at the substrate, the nuclei move freely in the drop and form at the end a disordered heap of crystals. These experiments thereby show that the preferential nucleation of the salt at the triple line is the second decisive parameter of the inclined or hollow rim formation, beside the outward advection of the dissolved salt due to the triple line pinning.

These experiments are a new proof of the potentiality of the wetting-growth coupling for surface patterning. This interplay is particularly noteworthy here because it takes place with a common liquid, on a common solid, in ambient conditions, contrary to the nanotube or nanowire manufacturing case, using refined materials in vacuum at high temperature [35, 36]. The number of conceivable applications of this surface-patterning techniques seems high, provided that a thorough optimization of the parameters is carried out, and that adapted solid/solvent couples are selected.

Acknowledgments

We thank Olivier Pierre-Louis for enlightening discussions, Charlotte Rivière, Agnès Piednoir and François Gay for experimental help and CNES (french space agency) and CNRS for financial support.

References

- [1] M. Diarra, A. Zappelli, H. Amara, F. Ducastelle, C. Bichara, Importance of carbon solubility and wetting properties of nickel nanoparticles for single wall nanotube growth, *Phys. Rev. Lett.* 109 (2012) 185501.
- [2] D. Zang, S. Tarafdar, Y. Y. Tarasevich, M. D. Choudhury, T. Dutta, Evaporation of a droplet: From physics to applications, *Phys. Rep.* 804 (2019) 1–56.
- [3] R. Deegan, O. Bakajin, T. Dupont, G. Huber, S. Nagel, T. Witten, Capillary flow as the cause of ring stains from dried liquid drops, *Nature* 389 (1997) 827.
- [4] Y. Li, C. Lv, Z. Li, D. Quéré, Q. Zheng, From coffee rings to coffee eyes, *Soft Matter* 11 (2015) 4669–4673.
- [5] X. Man, M. Doi, Ring to mountain transition in deposition pattern of drying droplets, *Phys. Rev. Lett.* 116 (2016) 066101.
- [6] B. Shin, M. Moon, H. Kim, Rings, igloos, and pebbles of salt formed by drying saline drops, *Langmuir* 30 (2014) 12837.
- [7] Y. Chen, K. Suzuki, H. Mahara, K. Yoshikawa, T. Yamaguchi, Self-organized archimedean spiral pattern: Regular bundling of fullerene through solvent evaporation, *Appl. Phys. Lett.* 102 (2013) 041911.

- [8] C. Annarelli, J. Fornazero, J. Bert, J. Colombani, Crack patterns in drying protein solution drops, *Eur. Phys. J. E* 5 (2001) 599.
- [9] K. A. Baldwin, M. Granjard, D. I. Willmer, K. Sefiane, D. J. Fairhurst, Drying and deposition of poly(ethylene oxide) droplets determined by péclet number, *Soft Matter* 7 (2011) 7819.
- [10] L. Pauchard, C. Allain, Stable and unstable surface evolution during the drying of a polymer solution drop, *Phys. Rev. E* 68 (2003) 052801.
- [11] F. Wang, S. Tian, Q. Yuan, Evaporation-induced crystal self-assembly (eicsa) of salt drops regulated by trace of polyacrylamide, *Colloids Surf. A* 644 (2022) 128856.
- [12] T. Yakhno, Salt-induced protein phase transitions in drying drops, *J. Colloid Interf. Sci.* 318 (2008) 225.
- [13] Y. Tarasevich, I. Vodolazskaya, O. Bondarenko, Modeling of spatial-temporal distribution of the components in the drying sessile droplet of biological fluid, *Colloids Surf. A* 432 (2013) 99.
- [14] B. Sobac, D. Brutin, Desiccation of a sessile drop of blood: Cracks, folds formation and delamination, *Colloids Surf. A* 448 (2014) 34.
- [15] C. Sadek, L. Pauchard, P. Schuck, Y. Fallourd, N. Pradeau, C. L. Floch-Fouéré, R. Jeantet, Mechanical properties of milk protein skin layers after drying: Understanding the mechanisms of particle formation from whey protein isolate and native phosphocaseinate, *Food Hydrocolloids* 48 (2015) 8.
- [16] P. Sáenz, A. Wray, Z. Che, O. Matar, P. Valluri, J. Kim, K. Sefiane, Dynamics and universal scaling law in geometrically-controlled sessile drop evaporation, *Nature Comm.* 8 (2017) 14783.
- [17] R. Cordeiro, T. Pakula, Behavior of evaporating droplets at nonsoluble and soluble surfaces: modeling with molecular resolution, *J. Phys. Chem. B* 109 (2005) 4152.
- [18] A. Mailleur, C. Pirat, O. Pierre-Louis, J. Colombani, hollow rims from water drop evaporation on salt substrates, *Phys. Rev. Lett.* 121 (2018) 214501.
- [19] D. Brutin, V. Starov, Recent advances in droplet wetting and evaporation, *Chem. Soc. Rev.* 47 (2018) 558.
- [20] H. Hu, R. Larson, Evaporation of a sessile droplet on a substrate, *J. Phys. Chem. B* 106 (2002) 1334–1344.
- [21] F. Carle, S. Semenov, M. Medale, D. Brutin, Contribution of convective transport to evaporation of sessile droplets: Empirical model, *Int. J. Thermal Sci.* 101 (2016).

- [22] R. Deegan, O. Bakajin, T. Dupont, G. Huber, S. Nagel, T. Witten, Contact line deposits in an evaporating drop, *Phys. Rev. E* 62 (2000) 756.
- [23] M. Moore, D. Vella, J. Oliver, The nascent coffee ring: How solute diffusion counters advection, *J. Fluid Mech.* 920 (2021) A54.
- [24] J. Colombani, Dissolution measurement free from mass transport, *Pure Appl. Chem.* 85 (2013) 61.
- [25] R. Arvidson, A. Luttge, Mineral dissolution kinetics as a function of distance from equilibrium – new experimental results, *Chem. Geol.* 269 (2010) 79.
- [26] B. Zareepolgaerdani, A. Piednoir, J. Colombani, Gypsum dissolution rate from atomic step kinetics, *J. Phys. Chem. C* 121 (2017) 9325.
- [27] A. Pachon-Rodriguez, A. Piednoir, J. Colombani, Pressure solution at the molecular scale, *Phys. Rev. Lett.* 107 (2011) 146102.
- [28] C. Fischer, R. Arvidson, A. Luttge, How predictable are dissolution rates of crystalline material?, *Geochim. Cosmochim. Acta* 98 (2012) 177.
- [29] A. A. Chernov, Step bunching and solution flow, *J. Optoelectron. Adv. Mater.* 5 (2003) 575.
- [30] N. Shahidzadeh-Bonn, S. Rafai, D. Bonn, G. Wegdam, Salt crystallization during evaporation: Impact of interfacial properties, *Langmuir* 24 (2008) 8599.
- [31] N. Shahidzadeh, M. Schut, J. Desarnaud, M. Prat, D. Bonn, Salt stains from evaporating droplets, *Scientific Reports* 5 (2015) 10335.
- [32] A. Giri, M. D. Choudhury, T. Dutta, S. Tarafdar, Multifractal growth of crystalline NaCl aggregates in a gelatin medium, *Crystal Growth Des.* 13 (2012) 341–345.
- [33] S. Kaneko, I. Hirasawa, Growth mechanism of hollow sodium chloride single crystals grown from a mixed solvent of cyclohexane and acetone, *Chem. Eng. Technol.* 40 (2017) 1276–1281.
- [34] J. Desarnaud, H. Derluyn, J. Carmeliet, D. Bonn, N. Shahidzadeh, Hopper growth of salt crystals, *J. Phys. Chem. Lett.* 9 (2018) 2961.
- [35] P. Yang, H. Yan, S. Mao, R. Russo, J. Johnson, R. Saykally, N. Morris, J. Pham, R. He, H. J. Choi, Controlled growth of zno nanowires and their optical properties, *Adv. Funct. Mater.* 12 (2002) 323.
- [36] K. Schwarz, J. Tersoff, From droplets to nanowires: dynamics of vapor-liquid-solid growth, *Phys. Rev. Lett.* 102 (2009) 206101.